ACS APPLIED MATERIALS & INTERFACES

Research Article

www.acsami.org

Creating Air-Stable Supported Lipid Bilayers by Physical Confinement Induced by Phospholipase A_2

Chung-Ta Han and Ling Chao*

Department of Chemical Engineering, National Taiwan University, Taipei 10617, Taiwan

Supporting Information

ABSTRACT: Supported lipid bilayer platforms have been used for various biological applications. However, the lipid bilayers easily delaminate and lose their natural structure after being exposed to an air−water interface. In this study, for the first time, we demonstrated that physical confinement can be used instead of chemical modifications to create air-stable membranes. Physical confinement was generated by the obstacle network induced by a peripheral enzyme, phospholipase A_2. The enzyme and reacted lipids could be washed away from the obstacle network, which was detergent-resistant and strongly bonded to the solid support. On the basis of these properties, the obstacle framework on the solid support was reusable and lipid bilayers with the desired composition could be refilled and formed in the region confined by the obstacle framework. The results of fluorescence recovery after photobleaching (FRAP) indicate that the diffusivities of the lipid bilayers before drying and after rehydration were comparable, indicating the air stability of the physically confined membrane. In addition, we observed that the obstacles could trap a thin layer of water after the air−water interface passed through the lipid bilayer. Because the obstacles were demonstrated to be several times higher than a typical lipid membrane on a support, the obstacles may act as container walls, which can trap water above the lipid membrane. The water layer may have prevented the air−water interface from directly contacting the lipid membrane and, therefore, buffered the interfacial force, which could cause membrane delamination. The results suggest the possibility of using physical confinement to create air-stable membranes without changing local membrane rigidity or covering the membrane with protecting molecules.

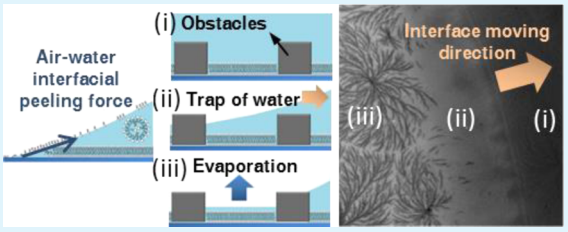

KEYWORDS: *lipid bilayers, air-stable, physical confinement, phospholipase A_2*

INTRODUCTION

Supported lipid bilayers (SLBs) have been considered as ideal biosensor platforms[1−3] and biocompatible coating materials.[4,5] An SLB can maintain two-dimensional fluidity by retaining a thin water layer between the solid support and the bilayer, thereby enabling the membrane-embedded species to move laterally in the bilayer plane. In addition, the bilayer structure can maintain the orientation of membrane-associated species to interact with other biomolecules. Both the fluidity and orientation are crucial properties for numerous cellular process interactions to occur. In addition, the zwitterionic property of the lipid bilayer makes it an ideal antifouling surface, thus enabling the SLB to become a potentially suitable biocompatible coating material. However, conventional SLBs easily delaminate after being exposed to an air−water interface. During the use of numerous bioapplications, the samples are inevitably exposed to air during transport, or reagent addition or exchange. Developing methods to form air-stable SLBs is critical for broadening the applications of SLBs.

The reason for delamination is that the air−water interface in contact with the lipid bilayer can provide an interfacial force, in the direction with an angle from the support, to break the bilayer structure and peel the bilayer from the support. To overcome the destructive interfacial force, numerous researchers have made attempts to increase the lipid membrane rigidity by modifying the surface chemistry of the solid support through the use of chemically modified lipids or by adding protection layers. The first method involves modifying the solid support surface by using the tethered cholesteryl group,[6] zirconium phosphate,[7,8] γ-aminopropylsaline,[9−11] or negatively charged poly(dimethylsiloxane) (PDMS)[1] to provide strong interactions between the supports and the lipid bilayers to overcome the interfacial peeling force. Another method involves the use of polymerizable lipids to cross-link the lipid bilayer structure[12−14] or lipopolymers, lipids with polymers attached to the head groups, to increase the rigidity and the degree of hydration of the membrane.[15] The other method involves the addition of biomolecules, such as proteins[16,17] and disaccharides,[18−23] to form protection layers above the membrane to enhance the bending modulus of the membrane and prevent the lipid bilayer from curling during delamination. Most of these methods enable the formation of air-stable membranes with promising stability and recoverable diffusion coefficients. However, strongly tethering the lipid membrane to the modified supports and modifying the lipid's chemical structure alters the native environment for certain membrane species,

Received: December 13, 2013
Accepted: April 10, 2014
Published: April 23, 2014

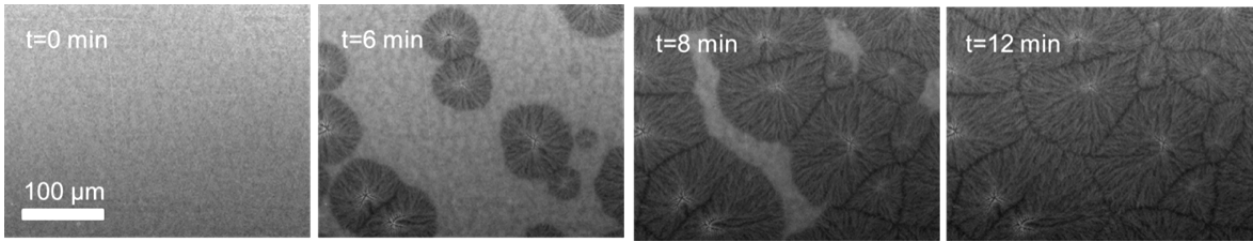

Figure 1. Morphology evolution of the obstacle network formation induced by PLA_2 (3.4 μg/mL) in a 40:40:20 DOPC/DPPC/Chol SLB. The incorporation of 0.5 mol % Texas-Red DHPE fluorescence lipid dye into the membrane revealed the multiple phases in the SLB.

and the addition of covering layers may cause steric hindrance and, consequently, block certain possible ligand–receptor interactions.

We intended to develop an air-stable membrane system based on a physical confinement mechanism. The major advantage of using physical confinement instead of increasing the membrane's rigidity is that the membrane property and its accessibility to the outside environment may not require considerable alteration. Previous studies have reported that several physical obstacles can appear on SLBs after phospholipase A_2 (PLA_2) hydrolysis in a multicomponent SLB system.[24−28] PLA_2 is an enzyme that can hydrolyze phospholipids in the sn-2 position to form lysophosphocholine and fatty acid as products. Atomic force microscopy (AFM) revealed that these obstacles have a crystal-like structure and a height of 10−20 nm.[29] Although no direct evidence of the composition of these crystal-like domains is available, previous studies have suggested that these obstacles could be composed of the enzyme's hydrolysis products.[24−26]

Herein, we prove that the lipid bilayers confined by the physical obstacles produced by PLA_2 can tolerate the air–water interface and maintain diffusivity and fluidity after rehydration. We demonstrated how to form the obstacle network on a solid support, clean the enzymes and residual lipids, and refill the desired lipid membranes in the region confined by the obstacles. The fluorescence recovery after photobleaching (FRAP) technique was used to examine the membrane fluidity before drying and after rehydration. In addition, we directly tracked the movement of the air–water interface by using bright-field and fluorescence microscopy to reveal the possible air-stable mechanism.

EXPERIMENTAL SECTION

Materials. 1,2-Dioleoyl-*sn*-glycero-3-phosphocholine (DOPC), 1,2-dipalmitoyl-*sn*-glycero-3-phosphocholine (DPPC), and cholesterol (Chol) were purchased from Avanti Polar Lipids (Alabaster, AL). Texas-Red 1,2-dihexadecanoyl-*sn*-glycero-3-phosphoethanolamine, triethylammonium salt (Texas-Red DHPE) was purchased from Life Technologies (Grand Island, NY). Phospholipase A_2 (PLA_2) from honey bee venom (*Apis mellifera*) was purchased from Sigma-Aldrich (St. Louis, MO).

Preparation of Obstacles Induced by PLA_2. The SLB in this work was formed using the vesicle deposition method. Large unilamellar vesicles (LUVs) comprising desired compositions were formed by using the previously introduced method.[30] Glass coverslips were cleaned using argon plasma for 10 min. A poly(dimethylsiloxane) (PDMS)-made well was rapidly sealed using the cleaned glass to generate a space to hold solutions above the glass coverslips. The prepared LUVs in a buffer (10 mM HEPES and 123 mM NaCl, pH = 7.4) were added to the glass area enclosed by the PDMS well. After 10 min of incubation to achieve vesicle deposition, the excessive lipid vesicles were washed away with deionized water. Subsequently, a Ca-HEPES buffer (10 mM HEPES, 123 mM NaCl, and 2.5 mM $CaCl_2$, pH = 7.4) was used to rinse the entire well to make the bulk solution environment suitable for the subsequent PLA_2 reaction.

A PLA_2 solution was added to the prepared SLBs, and the concentration of the enzyme was controlled at 3.4 μg/mL (113 nM). The sample was then incubated for 30 min with the PLA_2 solution to form a branch obstacle network. The sample containing branch obstacles was then immersed in a conical tube filled with a 0.1 M sodium dodecylsulfate (SDS) solution to wash away the remaining PLA_2 on the SLB surface and the lipid bilayers, except for the branch obstacles. The tube was sonicated for 30 min at 30 °C. After removal of the sample from the SDS solution, the sample was washed with water intensively for approximately 2 min. The sample was then passed through the air–water interface several times to ensure that SDS and the SLBs, except the branch obstacles, were washed away completely.

Preparation of Refilled Membranes in the Region Confined by the Obstacle Network. Fresh lipid vesicles (DOPC with 0.5 mol % Texas-Red DHPE) were added to the cleaned glass slide with the branch obstacle network. The lipid vesicles were deposited in the region where no obstacles were present. After 10 min of incubation to achieve vesicle deposition, the excessive lipid vesicles were washed away with deionized water.

Dehydration and Rehydration of the SLB. Most of the water in the PDMS well was removed using a pipet before dehydration. The sample was then placed in a Petri dish open to the atmosphere for approximately 1 h to allow the air–water interface moving front to appear. The phenomenon that occurred near the moving front was subsequently examined using fluorescence and bright-field microscopy. The start of the dry state was defined as the time immediately after the air–water interface just passed through the entire membrane sample. Water was added to rehydrate the sample at several specified time points after the dry state started.

Fluorescence Microscopy and FRAP. The lipid bilayer sample was exposed to a 200 mW DPSS Green Laser Module (Unice, Taiwan) at 532 nm to photobleach Texas-Red DHPE for 0.1 s. The bleached spot was a Gaussian profile that was approximately 10 μm in half-maximum width. The recovery images were taken using an inverted microscope (Olympus IX81, Olympus, Japan) equipped with a charge-coupled device camera (ORCA-R2, Hamamatsu, Japan) under a 20× objective lens (UPLSAPO, Olympus, Japan). The recovery evolution images were recorded, and the intensity recovery data inside the region of interest were fitted using *MATLAB* (Mathworks, Natick, MA) to calculate the diffusion coefficient of the SLB. The fitting algorithm was primarily based on the algorithm developed by Axelrod et al.[31] Details are provided in the Supporting Information (SI).

RESULTS AND DISCUSSION

Formation of an Obstacle Network Induced by PLA_2. Figure 1 shows the obstacle network growth when we applied PLA_2 (3.4 μg/mL, 113 nM) to SLBs with a 40:40:20 molar ratio of DOPC/DPPC/Chol. We incorporated 0.5 mol % Texas-Red DHPE fluorescence lipid dye into the membrane to reveal the process of morphology evolution. Before the addition of PLA_2, the preexisting dark domains are probably due to the phase separation of the liquid-ordered and liquid-disordered

dx.doi.org/10.1021/am405746g | ACS Appl. Mater. Interfaces 2014, 6, 6378−6383

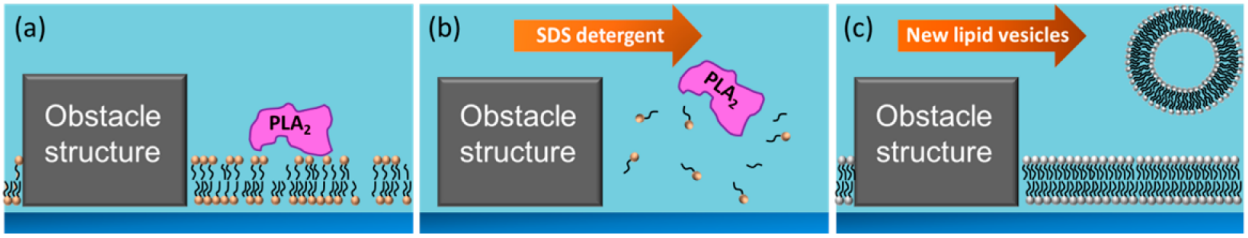

Figure 2. Procedure used to form SLBs with a desired composition in the region confined by the PLA_2-induced obstacle network: (a) situation after the obstacle network was induced by PLA_2; (b) removal of the enzyme and lipid residues by using SDS detergent and water; (c) formation of new SLBs in the free space by adding lipid vesicles with a desired composition.

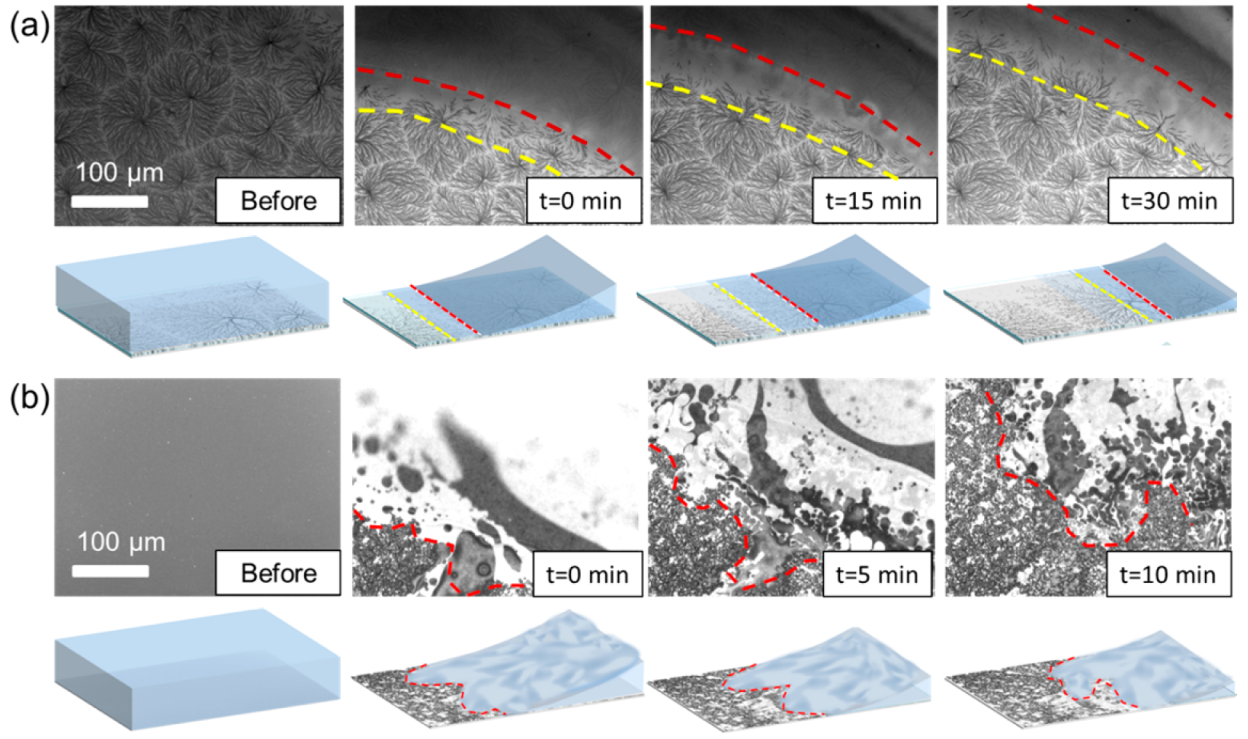

Figure 3. Direct observation of membrane morphology changes when the air−water interface passed through the membrane. (a) Fluorescence morphology evolution images and schematic illustrations of the SLB (DOPC with 0.5 mol % Texas-Red DHPE) with an obstacle network. (b) Evolution images and illustration of the SLB without an obstacle network. The red dashed lines indicate the major air−water interface fronts, which moved from the bottom-left to the upper-right corners of the images. The yellow dashed lines in part a were used to bind the region where part of the obstacle network still had not been revealed. t = 0 was set at the time when the evolution image series started to be recorded.

phases in the 40:40:20 DOPC/DPPC/Chol membrane at 23 °C, as reported previously.[32,33] After the addition of PLA_2, several new dark branch obstacles began to nucleate from various sites in the SLB, and the obstacle network continued growing radially from each nucleation site. At the end, the obstacles growing from various nucleation sites did not crossover, and the morphology reached a steady state after the entire region was occupied by the obstacle network.

Cleaning Residues and Refilling New Lipid Membranes in the Region Confined by the Obstacle Network. After formation of the obstacle network, we removed PLA_2 and the reacted lipid membrane from the sample, so that we can form the new lipid membrane with a desired composition in the region confined by the obstacle network. As illustrated in Figure 2, the sample was treated with 0.1 M SDS, and most of the lipid membrane dissolved and was removed from the support. However, the AFM results (in the SI) indicated that the obstacle network still remained on the glass solid support after being washed with detergent and contained stepwise plateaus with heights of approximately 12 and 20 nm, which was consistent with the results of previous studies that have reported that the height of the crystal-like structure is several times the height of a typical lipid bilayer.[29] The new lipid membrane with a desired composition (DOPC with 0.5 mol % Texas-Red DHPE) was subsequently used to refill the empty space, which was not covered by the obstacles. The similar shape and density of the obstacle network before the detergent wash and after the refill suggests that the obstacle network can remain on the support during the cleaning procedure (details in the SI, Figure S1). In addition, we determined that the branch obstacle can still remain on the support even after several SDS washes and water rinsing cycles, suggesting that the framework of the obstacle on the solid support is reusable.

Using Fluorescence Microscopy To Track the Air−Water Interface Moving Front. To examine how the lipid membrane formed in the region confined by the obstacle network could survive after being exposed to the air−water

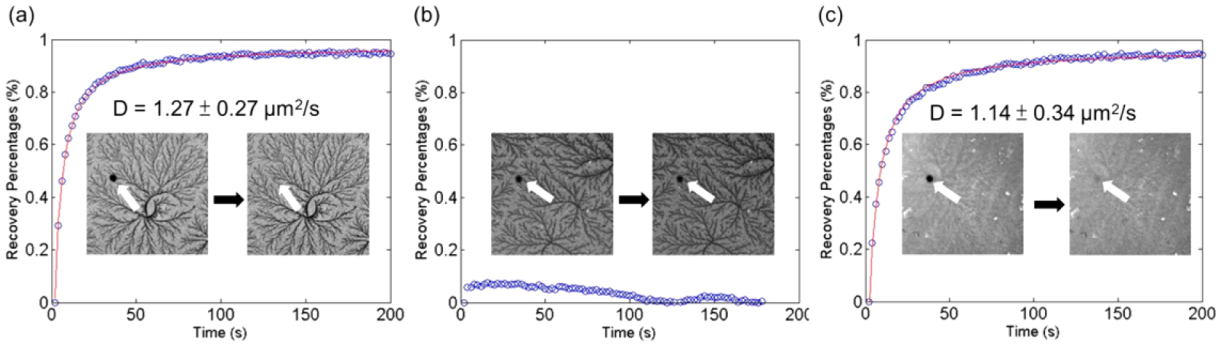

Figure 4. Fluorescence intensity recovery data (blue dots) and the fitted curves (red lines) used to obtain the diffusion coefficients of the SLB (DOPC with 0.5 mol % Texas-Red DHPE) with an obstacle network (a) before drying, (b) after drying, and (c) after rehydration. The inset fluorescence images were taken at the time points immediately after photobleaching and at the end of the recording. The white arrows indicate the locations of the bleached spots.

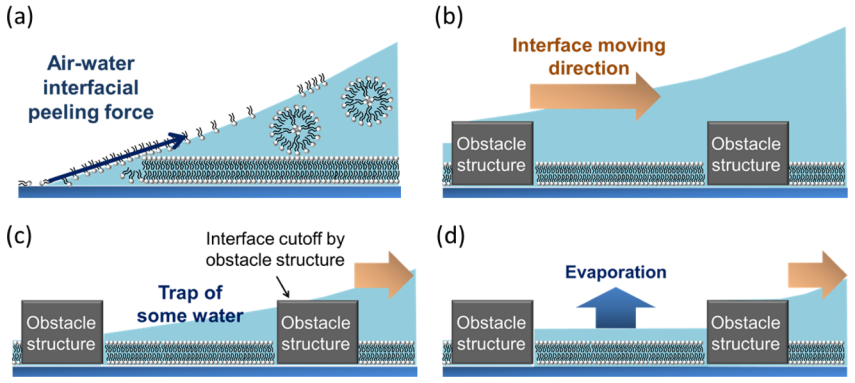

Figure 5. Illustration of how the obstacle network structure could prevent the air−water interface from directly coming into contact with the lipid membrane. (a) By not protecting and modifying the SLB, the air−water interface can directly come into contact with the SLB and produce a peel-off force. (b) The air−water interface front moved from the left to the right of the SLB with the obstacle network, (c) water may be left in the region confined by the obstacle network, and (d) the remaining water layer on the SLB eventually evaporates from the surface, and no considerable interfacial force in the peel-off direction can be directly applied to the membrane.

interface, we directly tracked the movement of the air−water interface during the dehydration process by using fluorescence microscopy. Figure 3a shows the morphology evolution images of the fluorescently labeled SLB confined in the obstacle network upon drying as the air−water interface moved from the bottom-left to the top-right corners. The SLB with an obstacle network did not delaminate and maintained its integrity. Conversely, delamination occurred easily in a typical fluid SLB sample after it was exposed to the air−water interface, as shown in Figure 3b. Delamination of the SLB resulted in the formation of bright lipid debris in the solution, whereas the solution above the SLB sample confined in the obstacle network remained transparent and clean. The fluorescence images suggest that the SLB confined in the obstacle network remained considerably intact after being exposed to the air−water interface.

Furthermore, the obstacle network seemed to retain a thin water layer after the air−water interface passed through the membrane (Figure 3a; the movie clip of this process is included in the SI). We defined the air−water interface moving front as the visible line in the image caused by the substantial change in light refraction at the water moving front (highlighted by red dashed lines; original images in the SI). We observed that part of the obstacle network was not immediately revealed after the defined air−water interface front had passed, as shown in the region bounded by the red and yellow dashed lines in Figure 3a. We hypothesized that these unrevealed objects were still covered by water because the objects immersed under water or exposed to air could have considerably different microscope focusing planes as a result of the distinct light refractive indexes of air and water. The dark obstacle network was revealed later most likely because the thin water layer covering the obstacle network evaporated over time. The partial concealment was most likely caused by the uneven height of the obstacles, which caused several obstacles to be covered by water, whereas the others were already exposed to air. We did not observe the water retention phenomenon in the SLB without the obstacle network (Figure 3b). The results suggest that the obstacle network may be able to buffer the interfacial peeling force by trapping a thin water layer above the lipid bilayer confined in the obstacle network.

Using FRAP To Examine the Membrane Integrity before Drying, after Drying, and after Rehydration. The FRAP technique involves the use of a laser to bleach fluorescent molecules in a small region of a sample, and the diffusion coefficient can be obtained by analyzing the fluorescence recovery over time in this small region.[31] Figure 4 shows the fluorescence images of the membrane morphology and the normalized recovery intensity data before drying, after drying, and after rehydration. The fitted curves indicate that the diffusion coefficient before dehydration was 1.27 ± 0.27 $\mu m^2/s$ and the recovery percentage was 95% (as a reference, the measured diffusion coefficient of 99.5 mol % DOPC/0.5 mol % Texas-Red DHPE SLB without an obstacle network was 1.87 ±

0.18 $\mu m^2/s$ in this system). After the sample was dehydrated, the recovery percentage was negligible. After rehydration, the diffusion coefficient was 1.14 ± 0.34 $\mu m^2/s$ and the recovery percentage was approximately 95%. The recovery situation can be observed in the inset fluorescence images, which show the bleached spot at the beginning of the bleaching process and at the end of the recording. The comparable measured diffusion coefficients before dehydration and after rehydration suggest that the lipid membrane maintained its integrity after it came into contact with the air−water interface and rehydrated.

We observed that the diffusion coefficients of the rehydrated bilayers were influenced by the time duration when the bilayers remained dry. The membrane that was rehydrated after it was maintained in a dry state for 1 h had almost the same diffusion coefficient as that of the membrane before drying. The diffusion coefficient of the 5-day-dry-state rehydrated membrane became almost half of the diffusion coefficient of the 1-h-dry-state rehydrated membrane (details in the SI). We determined the start of the dry state at the time immediately after the air−water interface passed through the entire membrane sample. The FRAP data shown in Figure 4b were obtained from the sample approximately 1 h after the dry state started, and the poor fluorescence recovery supports the theory that the water was removed because the lipid could no longer laterally diffuse in the bilayer. These observations suggest that, although the bilayer can be prevented from being destroyed by the interfacial force, the bilayer structure may not be stable when exposed to air for a long time. Degradation of the bilayer structure may be the limitation of using this method for assays requiring long air-exposure time. However, this method is still highly useful for conducting certain bioassays in which air bubbles are inevitably introduced during the reagent exchange and for applications that do not require the samples to leave aqueous solutions for a long time.

Possible Air-Stable Mechanism as a Result of Physical Confinement. Figure 5 illustrates the possible air-stable mechanism of the SLB with the obstacle network. We observed that a layer of water remained after the air−water interface passed through the sample and the obstacle network structure was several times higher than a typical 5 nm lipid membrane. On the basis of the observations, we hypothesized that the obstacles could act as containers to trap water inside the region confined by them to prevent the air−water interfacial force from coming into direct contact with the lipid membrane on the solid support. Typically, without any protection and modification of the SLB, the air−water interface can directly come into contact with the SLB and produce a peel-off force, as shown in Figure 5a. The force component perpendicular to the solid support could break the interaction between the lipid bilayer and the solid support, and the force component parallel to the lipid bilayer could break the van der Waals force between the lipid molecules. Therefore, an SLB may not be able to sustain the force and would subsequently delaminate. By contrast, if the obstacle network has a height higher than that of the SLB, it could protect the SLB from being directly exposed to the interfacial force, as illustrated in Figure 5b−d. As the air−water interface front moves, water may remain in the region confined by the obstacle network. Although the small amount of the remaining water layer on the SLB would eventually evaporate from the surface, no considerable interfacial force in the peel-off direction would be directly applied to the membrane. The SLB could preserve both its integrity and fluidity after being dried and rehydrated.

Note that the water front moving angle and the distance between the obstacle branches would determine whether water can be trapped in the space between the branches. For the case shown in this study, the distance between the branches in the obstacle network is at the micrometer scale and the height was approximately tens of nanometers. For water to be trapped in the obstacle network, the contact angle must be near 0°, which is consistent with our observations. We also used a PLA_2 concentration that was lower than the typical concentration we used in order to obtain a sparser obstacle network. When the sparser network was applied, we observed that several fluorescently labeled lipid bilayers peeled off and fluorescence lipid debris was produced in the solution (details in the SI). This result supports the proposed mechanism in which the moving front angle and the distance between the obstacle branches play crucial roles in determining the air stability. We are currently further exploring the required network density and moving front velocity criteria for this air-stability mechanism to robustly work under various conditions.

CONCLUSION

Creating SLBs that are insensitive to the air−water interface while the typical membrane properties are maintained is desirable. Conventional chemical methods can be used to achieve air stability by increasing the membrane rigidity and, thus, influence the membrane properties, which could be crucial for detecting certain biological phenomena. We used the physical confinement developed in this study to achieve air stability by trapping a water layer to buffer the air−water interfacial force, instead of changing the membrane rigidity to overcome the force. We demonstrated how to form the obstacle network on a solid support by using an enzyme, PLA_2, to clean the enzymes and residual lipids and to refill the desired lipid membranes. The FRAP data suggested that the membrane fluidity and integrity before drying and after rehydration were similar. In addition, the obstacles seemed to be inert, and the membrane diffusion coefficient was similar to that of a typical SLB. Although the fluid membrane connectivity, which was larger than the micrometer scale, may have been hindered by the obstacles, the unaltered local membrane property would be beneficial for numerous biosensing applications that require only biomolecule interactions at a length scale that is much smaller than the micrometer scale.

ASSOCIATED CONTENT

Supporting Information

Fluorescence recovery after photobleaching data analysis, control experiments, some detailed characterizations of a PLA_2-induced obstacle network, and movie clips of Figure 3a,b. This material is available free of charge via the Internet at http://pubs.acs.org.

AUTHOR INFORMATION

Corresponding Author

*E-mail: lingchao@ntu.edu.tw.

Notes

The authors declare no competing financial interest.

ACKNOWLEDGMENTS

We thank the National Science Council in Taiwan for funding support for this work (Grant NSC102-2221-E-002-153-MY3).

ABBREVIATIONS

DOPC = 1,2-dioleoyl-*sn*-glycero-3-phosphocholine; DPPC = 1,2-dipalmitoyl-*sn*-glycero-3-phosphocholine; Chol = cholesterol; Texas-Red DHPE = 1,2-dihexadecanoyl-*sn*-glycero-3-phosphoethanolamine, triethylammonium salt; PLA_2 = phospholipase A_2

REFERENCES

(1) Phillips, K. S.; Dong, Y.; Carter, D.; Cheng, Q. Stable and Fluid Ethylphosphocholine Membranes in a Poly(dimethylsiloxane) Microsensor for Toxin Detection in Flooded Waters. *Anal. Chem.* **2005**, *77* (9), 2960−2965.

(2) Castellana, E. T.; Cremer, P. S. Solid Supported Lipid Bilayers: From Biophysical Studies to Sensor Design. *Surf. Sci. Rep.* **2006**, *61* (10), 429−444.

(3) Jonsson, M. P.; Jönsson, P.; Dahlin, A. B.; Höök, F. Supported Lipid Bilayer Formation and Lipid-Membrane-Mediated Biorecognition Reactions Studied with a New Nanoplasmonic Sensor Template. *Nano Lett.* **2007**, *7* (11), 3462−3468.

(4) Chen, S.; Zheng, J.; Li, L.; Jiang, S. Strong Resistance of Phosphorylcholine Self-Assembled Monolayers to Protein Adsorption: Insights into Nonfouling Properties of Zwitterionic Materials. *J. Am. Chem. Soc.* **2005**, *127* (41), 14473−14478.

(5) Chapman, D. Biomembranes and New Hemocompatible Materials. *Langmuir* **1993**, *9* (1), 39−45.

(6) Deng, Y.; Wang, Y.; Holtz, B.; Li, J.; Traaseth, N.; Veglia, G.; Stottrup, B. J.; Elde, R.; Pei, D.; Guo, A.; Zhu, X. Y. Fluidic and Air-Stable Supported Lipid Bilayer and Cell-Mimicking Microarrays. *J. Am. Chem. Soc.* **2008**, *130* (19), 6267−6271.

(7) Oberts, B. P.; Blanchard, G. J. Formation of Air-Stable Supported Lipid Monolayers and Bilayers. *Langmuir* **2009**, *25* (5), 2962−2970.

(8) Fabre, R. M.; Talham, D. R. Stable Supported Lipid Bilayers on Zirconium Phosphonate Surfaces. *Langmuir* **2009**, *25* (21), 12644−12652.

(9) Fang, Y. Air stability of Supported Lipid Membrane Spots. *Chem. Phys. Lett.* **2011**, *512* (4−6), 258−262.

(10) Fang, Y. Spreading and Segregation of Lipids in Air-Stable Lipid Microarrays. *J. Am. Chem. Soc.* **2006**, *128* (10), 3158−3159.

(11) Fang, Y.; Frutos, A. G.; Lahiri, J. Membrane Protein Microarrays. *J. Am. Chem. Soc.* **2002**, *124* (11), 2394−2395.

(12) Ross, E. E.; Bondurant, B.; Spratt, T.; Conboy, J. C.; O'Brien, D. F.; Saavedra, S. S. Formation of Self-Assembled, Air-Stable Lipid Bilayer Membranes on Solid Supports. *Langmuir* **2001**, *17* (8), 2305−2307.

(13) Halter, M.; Nogata, Y.; Dannenberger, O.; Sasaki, T.; Vogel, V. Engineered Lipids That Cross-Link the Inner and Outer Leaflets of Lipid Bilayers. *Langmuir* **2004**, *20* (6), 2416−2423.

(14) Conboy, J. C.; Liu, S.; O'Brien, D. F.; Saavedra, S. S. Planar Supported Bilayer Polymers Formed from Bis-Diene Lipids by Langmuir−Blodgett Deposition and UV Irradiation. *Biomacromolecules* **2003**, *4* (3), 841−849.

(15) Albertorio, F.; Diaz, A. J.; Yang, T.; Chapa, V. A.; Kataoka, S.; Castellana, E. T.; Cremer, P. S. Fluid and Air-Stable Lipopolymer Membranes for Biosensor Applications. *Langmuir* **2005**, *21* (16), 7476−7482.

(16) Holden, M. A.; Jung, S.-Y.; Yang, T.; Castellana, E. T.; Cremer, P. S. Creating Fluid and Air-Stable Solid Supported Lipid Bilayers. *J. Am. Chem. Soc.* **2004**, *126* (21), 6512−6513.

(17) Dong, Y.; Phillips, K. S.; Cheng, Q. Immunosensing of Staphylococcus Enterotoxin B (SEB) in Milk with PDMS Microfluidic Systems Using Reinforced Supported Bilayer Membranes (r-SBMs). *Lab Chip* **2006**, *6* (5), 675−681.

(18) Albertorio, F.; Chapa, V. A.; Chen, X.; Diaz, A. J.; Cremer, P. S. The α,α-(1→1) Linkage of Trehalose Is Key to Anhydrobiotic Preservation. *J. Am. Chem. Soc.* **2007**, *129* (34), 10567−10574.

(19) Harland, C. W.; Botyanszki, Z.; Rabuka, D.; Bertozzi, C. R.; Parthasarathy, R. Synthetic Trehalose Glycolipids Confer Desiccation Resistance to Supported Lipid Monolayers. *Langmuir* **2009**, *25* (9), 5193−5198.

(20) Bennun, S. V.; Faller, R.; Longo, M. L. Drying and Rehydration of DLPC/DSPC Symmetric and Asymmetric Supported Lipid Bilayers: a Combined AFM and Fluorescence Microscopy Study. *Langmuir* **2008**, *24* (18), 10371−10381.

(21) Ricker, J. V.; Tsvetkova, N. M.; Wolkers, W. F.; Leidy, C.; Tablin, F.; Longo, M.; Crowe, J. H. Trehalose Maintains Phase Separation in an Air-Dried Binary Lipid Mixture. *Biophys. J.* **2003**, *84* (5), 3045−3051.

(22) Chiantia, S.; Kahya, N.; Schwille, P. Dehydration Damage of Domain-Exhibiting Supported Bilayers: An AFM Study on the Protective Effects of Disaccharides and Other Stabilizing Substances. *Langmuir* **2005**, *21* (14), 6317−6323.

(23) Oliver, A. E.; Kendall, E. L.; Howland, M. C.; Sanii, B.; Shreve, A. P.; Parikh, A. N. Protecting, Patterning, and Scaffolding Supported Lipid Membranes Using Carbohydrate Glasses. *Lab Chip* **2008**, *8* (6), 892−897.

(24) Grainger, D. W.; Reichert, A.; Ringsdorf, H.; Salesse, C. Hydrolytic Action of Phospholipase A_2 in Monolayers in the Phase Transition Region: Direct Observation of Enzyme Domain Formation Using Fluorescence Microscopy. *Biochim. Biophys. Acta, Biomembr.* **1990**, *1023* (3), 365−379.

(25) Maloney, K. M.; Grainger, D. W. Phase Separated Anionic Domains in Ternary Mixed Lipid Monolayers at the Air−Water Interface. *Chem. Phys. Lipids* **1993**, *65* (1), 31−42.

(26) Carlson, P. A.; Gelb, M. H.; Yager, P. Zero-order interfacial enzymatic degradation of phospholipid tubules. *Biophys. J.* **1997**, *73* (1), 230−238.

(27) Gudmand, M.; Rocha, S.; Hatzakis, N. S.; Peneva, K.; Müllen, K.; Stamou, D.; Uji-I, H.; Hofkens, J.; Bjørnholm, T.; Heimburg, T. Influence of Lipid Heterogeneity and Phase Behavior on Phospholipase A_2 Action at the Single Molecule Level. *Biophys. J.* **2010**, *98* (9), 1873−1882.

(28) Chibowski, E.; Holysz, L.; Jurak, M. Effect of a Lipolytic Enzyme on Wettability and Topography of Phospholipid Layers Deposited on Solid Support. *Colloids Surf., A* **2008**, *321* (1−3), 131−136.

(29) Balashev, K.; Atanasov, V.; Mitewa, M.; Petrova, S.; Bjornholm, T. Kinetics of Degradation of Dipalmitoylphosphatidylcholine (DPPC) Bilayers as a Result of Vipoxin Phospholipase A_2 Activity: an Atomic Force Microscopy (AFM) Approach. *Biochim. Biophys. Acta* **2011**, *1808* (1), 191−198.

(30) Lin, C. Y.; Chao, L. Tunable Nucleation Time of Functional Sphingomyelinase-Lipid Features Studied by Membrane Array Statistic Tool. *Langmuir* **2013**, *29* (42), 13008−13017.

(31) Axelrod, D.; Koppel, D. E.; Schlessinger, J.; Elson, E.; Webb, W. W. Mobility Measurement by Analysis of Fluorescence Photobleaching Recovery Kinetics. *Biophys. J.* **1976**, *16* (9), 1055−1069.

(32) Veatch, S. L.; Keller, S. L. Seeing Spots: Complex Phase Behavior in Simple Membranes. *Biochim. Biophys. Acta* **2005**, *1746* (3), 172−185.

(33) Davis, J. H.; Clair, J. J.; Juhasz, J. Phase Equilibria in DOPC/DPPC-d62/Cholesterol Mixtures. *Biophys. J.* **2009**, *96* (2), 521−539.